WPMAG-CPR(17) 18607

M. Lewandowska et al.

Thermal-hydraulic analysis of different design concepts of the LTS TF coil winding pack for EU-DEMO

Preprint of Paper to be submitted for publication in Proceeding of 9th International Conference Electromagnetic Devices and Processes in Environment Protection ELMECO-9 with 12th Seminar

This work has been carried out within the framework of the EUROfusion Consortium and has received funding from the Euratom research and training programme 2014-2018 under grant agreement No 633053. The views and opinions expressed herein do not necessarily reflect those of the European Commission.

Thermal-hydraulic Analysis of Different Design Concepts of the LTS TF Coil Winding Pack for EU-DEMO

Monika Lewandowska, Aleksandra Dembkowska
Faculty of Mechanical Engineering and Mechatronics
West Pomeranian University of Technology, Szczecin
Szczecin, Poland
monika.lewandowska@zut.edu.pl

Kamil Sedlak
Swiss Plasma Center (SPC)
École Polytechnique Fédérale de Lausanne (EPFL)
Villigen PSI, Switzerland
kamil.sedlak@psi.ch

***Abstract*— The new iteration of three design concepts of the low Tc superconductor winding pack for the EU-DEMO Toroidal Field (TF) coil has been proposed in 2016 by EPFL-SPC PSI Villigen, ENEA Frascati and CEA Cadarache. Our work presents the results of the thermal-hydraulic analysis of all the candidate designs using simplified models. The performed analysis includes: (i) hydraulic analysis – calculation of the mass flow rates in each conductor at the expected value of pressure drop in the coil at the operating conditions during the dwell phase, (ii) heat removal analysis aimed at the assessment of the minimum temperature margin at the end of the plasma burn, (iii) assessment of the maximum temperature and the maximum pressure in each conductor during quench for the extreme case of quench initiation. The influence of the nuclear heat load map, realistic magnetic field map and joint resistance on the value of the minimum temperature margin in WP#1 is studied in details.**

Keywords*— *EU-DEMO; tokamak; TF coil; temperature margin; quench

I. Introduction

Design and assessment studies on the European DEMOnstration Fusion Power Plant (EU DEMO), which should demonstrate feasibility of grid electricity production at the level of a few hundred MW by the middle of the present century, are carried out by the EUROfusion Consortium [1], [2]. The heart of DEMO will be a tokamak equipped with a superconducting magnet system. Recent efforts of the DEMO Magnet System project team were focused mainly on further refinement and improvement of different concepts of the Toroidal Field (TF) coil design, but also the conceptual studies on the Central Solenoid (CS) design were initiated [3]-[9]. According to the 2015 DEMO baseline [10], still valid in 2016, the TF system will consist of 18 TF coils. The new iteration of three design concepts of the low T_c superconductor (LTS) winding pack (WP) for the DEMO TF coil, namely WP#1, 2 and 3, has been proposed in 2016 by EPFL-SPC PSI Villigen, ENEA Frascati and CEA Cadarache, respectively. According to these concepts the TF coil is composed of: (i) WP#1 (SPC) design: 12 single layers (Ls) wound using flat multistage Nb3Sn React and Wind (R&W) cables with two side equilateral triangle cooling channels and one rectangular cooling channel [4] (Fig. 1a); (ii) WP#2 (ENEA) design: 6 double layers (DLs) wound using rectangular Cable-in-Conduit Conductors (CICCs) with two spiral cooling channels [5] (Fig. 2a), 5 inner DLs are made of Nb_3Sn Wind and React (W&R) cables, whereas the outermost DL, located in low magnetic field region, utilizes NbTi; (iii) WP#3 (CEA) design: 9 double pancakes (DPs) wound using a square Nb_3Sn W&R CICC with a central spiral cooling channel [6] (Fig. 1c).

This work was carried out within the framework of the EUROfusion Consortium and was supported in part by the Euratom Research and Training Program 2014–2018 under Grant 633053 and in part by the Polish Ministry of Science and Higher Education within the framework of the financial resources in the years 2016-2017 allocated for the realization of the international cofinanced project. The views and opinions expressed herein do not necessarily reflect those of the European Commission.

Our present study is focused on the thermal-hydraulic analysis of all the WP concepts, aimed at the verification if the proposed conductor designs fulfil the acceptance criteria and at further development of the simplified models used as tools. It is a continuation of the earlier studies of the previous concepts of the DEMO coils designs [11]-[15].

II. Model Assumptions

Conductor parameters relevant for the present study are compiled in Tables I and II. Symbol L denotes the cable length (for WP#2 we specified the length of the inner conductor in each DL), A – the cross section of a cable component, D_h – the hydraulic diameter, φ - the bundle void fraction, $B_{eff\ max}$ – the maximum of the computed effective magnetic field, $T_{cs\ min}$ – minimum value of the current sharing temperature, calculated as $T_{cs}(B_{eff\ max})$. Index B represents the bundle region, sc – the superconductor, He – helium, *side* and *rect* – side and rectangular cooling channels in WP#1, respectively, $Cu1$ – copper component with RRR = 100 in superconducting strands, $Cu2$ – copper in segregated strands or in the outer shell (index sh) with RRR = 400, 450 or 300 in the WP#1, 2 or 3, respectively. The outer/inner diameters of the steel spirals delimiting the cooling channels from the bundle regions are equal to 5/7 mm and 8/10 mm in WP#2 and 3, respectively. The spirals in WP#2 are made of a strip with a width of 5 mm and have the open area of 40%, whereas the detailed geometry

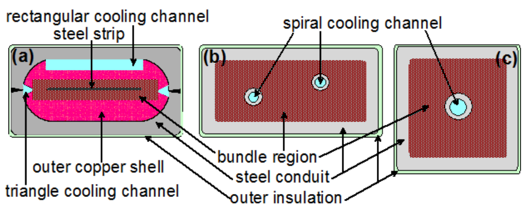

Fig. 1. Schematic cross section of a (a) WP#1, (b) WP#2, and (c) WP#3 conductor.

TABLE I. PARAMETERS of WP#1 (SPC DESIGN) CONDUCTORS USED IN THE PRESENT STUDY

Layer	L (m)	$A_{sc\,B}$ (mm^2)	$A_{Cu1\,B}$ (mm^2)	$A_{Cu2\,B}$ (mm^2)	$A_{He\,B}$ (mm^2)	$D_{h\,B}$ (mm)	φ (-)	$A_{He\,side}$ (mm^2)	$D_{h\,side}$ (mm)	$A_{He\,rect}$ (mm^2)	$D_{h\,rect}$ (mm)	$A_{Cu2\,sh}$ (mm^2)	A_{jacket} (mm^2)	$B_{eff\,max}$ (T)	$T_{cs\,min}$ (K)	Q_{NH1} (W)	Q_{NH2} (W)
1	846.6	146.0	146.0	16.2	79.4	0.536	0.20	16.0	2.48	140.0	7.18	474.7	943	12.26	6.72	36.1	43.7
2	850.8	115.9	115.9	12.9	63.1	0.448	0.20	16.0	2.48	140.0	7.18	507.3	966	11.21	6.82	28.1	37.4
3	855.1	93.9	93.9	10.4	51.1	0.403	0.20	16.0	2.48	140.0	7.18	531.2	1036	10.40	6.74	22.6	33.5
4	859.6	82.1	82.1	9.1	44.7	0.400	0.20	16.0	2.48	120.0	7.06	543.9	1153	9.75	6.79	18.3	31.0
5	864.1	70.0	70.0	23.3	42.1	0.424	0.20	16.0	2.48	115.0	7.02	541.9	1249	8.88	6.91	14.7	29.2
6	868.8	60.4	60.4	20.1	36.3	0.419	0.20	16.0	2.48	95.0	6.85	554.5	1378	8.19	6.90	11.8	28.0
7	873.7	50.7	50.7	16.9	30.5	0.418	0.20	16.0	2.48	85.0	6.73	567.0	1479	7.47	6.78	9.3	27.0
8	878.8	45.0	45.0	15.0	27.0	0.378	0.20	16.0	2.48	70.0	6.51	574.5	1607	6.93	6.73	7.3	26.8
9	883.8	43.0	43.0	14.3	25.9	0.377	0.20	16.0	2.48	60.0	6.32	577.0	1520	6.74	6.69	5.3	24.8
10	889.0	41.1	41.1	13.7	24.7	0.376	0.20	16.0	2.48	50.0	6.06	579.6	1684	6.58	6.61	4.2	25.6
11	894.3	39.1	39.1	13.0	23.5	0.374	0.20	16.0	2.48	40.0	5.71	582.1	1812	6.46	6.47	3.3	25.6
12	804.5	37.2	37.2	12.4	22.3	0.373	0.20	16.0	2.48	40.0	5.71	584.7	1133	6.14	6.54	1.7	19.3

TABLE II. PARAMETERS OF WP#2 AND WP#3 CONDUCTORS

No	L (m)	$A_{sc\,B}$ (mm^2)	$A_{Cu1\,B}$ (mm^2)	$A_{Cu2\,B}$ (mm^2)	$A_{He\,B}$ (mm^2)	$D_{h\,B}$ (mm)	φ (-)	$B_{eff\,max}$ (T)	$T_{cs\,min}$ (K)	Q_{NH1} (W)
WP#2 (ENEA DESIGN)										
L1	747	291.5	291.5	484.3	404.7	0.57	0.27	11.8	7.2	39.6
L3	755	145.7	145.7	679.4	330.3	0.54	0.25	9.9	7.0	23.9
L5	763	109.3	109.3	726.4	322.1	0.58	0.25	8.6	7.2	15.1
L7	773	72.9	72.9	702.9	287.2	0.56	0.25	7.2	7.0	8.7
L9	782	48.6	48.6	777.3	292.0	0.52	0.25	6.2	6.3	5.1
L11	794	302.7	484.3	192.8	414.7	0.59	0.29	5.7	6.3	3.0
WP#3 (CEA DESIGN)										
SP	408	329.8	333.1	632.4	524.3	0.55	0.29	11.7	6.2	11.68

of the central spiral in WP#3 has not been specified yet. The nominal operating current flowing in conductors is I_0 = 63.3 kA (WP#1), 70.8 kA (WP#2), or 88.146 kA (WP#3).

As in earlier studies [11]-[15], we assume that the TF coil is cooled by forced flow of supercritical helium at T_{in} = 4.5 K and p_{in} = 0.6 MPa. All cables in the coil are connected hydraulically in parallel and the expected value of pressure drop at normal operation conditions is Δp = 0.1 MPa.

As proposed in [16], the expected value of the nuclear heat (NH) load, deposited in the TF case and WP due to neutron irradiation, can be estimated by integrating the formula:

$$P_{NH1} = 50\ \mathrm{W/m^3}\cdot\exp(-r_{case}/0.140\ \mathrm{m}), \qquad (1)$$

where r_{case} is the radial distance from the TF case plasma-facing edge (see Fig. 2). Equation (1) served as a reference for

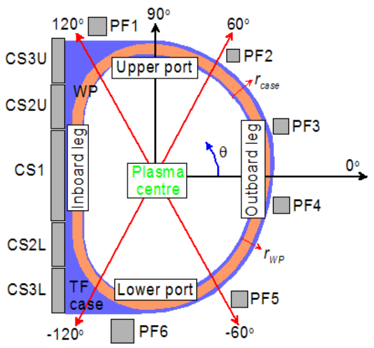

Fig. 2. The TF coil position with respect to other DEMO coils and the coordinates used in Eqs. (1) and (2).

the present WP design, so it will be retained as a basic approach in our analysis. However, the most recent neutronic study, carried out for the EU-DEMO 2015 baseline, revealed that (1) may underestimate the NH load in some parts of the TF coil, and the following more advanced formula for NH load in the WP was proposed in [17]:

$$P_{NH2}(\theta, r_{WP}, z) = \begin{cases} 10\ \mathrm{W/m^3} & \text{for } -60^\circ < \theta < 60^\circ \\ 10\ \mathrm{W/m^3}\cdot\exp(z/0.448\,\mathrm{m}) & \text{for } 60^\circ \le \theta \le 120^\circ \\ 50\ \mathrm{W/m^3}\cdot\exp(-r_{WP}/0.217\,\mathrm{m}) & \text{for } 120^\circ < \theta < -120^\circ \\ 10\ \mathrm{W/m^3}\cdot\exp(-r_{WP}/1\,\mathrm{m})\cdot\exp(z/0.448\,\mathrm{m}) & \text{for } -120^\circ \le \theta \le -60^\circ \end{cases}, \qquad (2)$$

where r_{WP} is the radial distance from the WP edge, θ is the angle in the vertical plane (Fig. 2) and z is the coordinate in the toroidal direction with z = 0 in the coil centre. We study the effect of the NH load map obtained with the new approach on the temperature margin (ΔT_{marg}) in WP#1 conductors.

We assume that in the layer wound coils (WP#1 and 2) the NH load is deposited evenly throughout each conductor, whereas in the pancake wound WP#3 heat deposited over each turn is different. The values of the total NH load directly deposited in conductors, Q_{NH1} and Q_{NH2}, obtained from (1) and (2), respectively, are compiled in last columns of Tables I and II. It is seen that Q_{NH2} is much larger than Q_{NH1}, particularly in the outer layers. For WP#1 and 2 we assume that the NH load absorbed in the case will be fully removed by a dedicated case cooling circuit. For WP#3 we study three scenarios: apart from the NH load directly deposited in conductors (Case **a**), we consider additional heat transfer from the uncooled case (Case **b**) or additional heat transfer from the case with cooling channels (Case **c**). The values of additional transient heat fluxes from the case, ensuing from the 2D Cast3M thermal calculations [9] were provided by the CEA team. We extracted from these data the values for the central, the most critical, pancake at the end of the plasma burn. The resulting NH load maps are presented in Fig. 3.

For WP#1cables, with the joint located at the inlet, we take into account an additional heat deposition due to the joint resistance R_{JR} = 1 nΩ. In the WP#3 conductors the joints will be located at the conductors' outlet, so the related heat load will not affect the temperature profiles in conductors. For WP#2 the joint location has not been specified yet. Thus, for

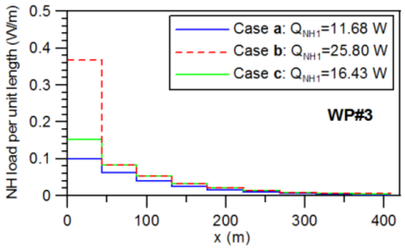

Fig.3. NH load maps used in the analysis of the WP#3 central pancake.

the WP#2 and 3 conductors heat load resulting from the joint resistance is not considered.

The performed analysis includes the following stages: (i) Hydraulic analysis – calculation of the mass flow rates in each channel of flow at the operating conditions during the dwell phase, i.e. assuming no heat load in conductors, based on the 1 D momentum balance equation; (ii) Heat removal analysis – calculation of the mass flow rates as well as temperature and pressure profiles in conductors at the expected NH load corresponding to the end of burn. The analysis is based on 1 D steady state energy and momentum balance equations and is aimed at the assessment of the minimum temperature margin; (iii) Assessment of the maximum quench temperature and pressure, based on the 0 D transient energy balance equation for the extreme pressure quench initiation scenario – whole conductor in quench and all channels of flow blocked. The applied methodology is described in detail in [11].

In the hydraulic analysis, for flow in bundle regions we use porous medium correlations f_{DF} and f_M developed in [18] and [19], respectively. For the non-circular cooling channels of the WP#1 conductors we used the Bhatti – Shah friction factor correlation f_{BS} for the turbulent flow in smooth tubes [20], for the spiral WP#2 cooling channels with known geometry the correlations f_{Zan1} [21] and f_{Zan2} [22] are applied, whereas for the WP#3 spiral cooling channel - the empirical correlation f_{spiral} taken from [15].

In the earlier studies [12]-[14] the minimum ΔT_{marg} was estimated conservatively in the simplified way as: $\Delta T^{\min}_{marg,s} = T_{cs\min} - T_{out}$ for the layer wound WP#1 and 2, or $\Delta T^{\min}_{marg,s} = T_{cs\min} - T(x_{crit})$ for the pancake wound WP#3, where x_{crit} was the expected critical point located at the end of the high field region in the first turn, which was every time specified by the WP#3 designers. In the present work we introduced to the heat removal model the realistic magnetic field map. The magnetic field profile along the WP#3 central pancake conductor was taken from [9], for the WP#1 cables

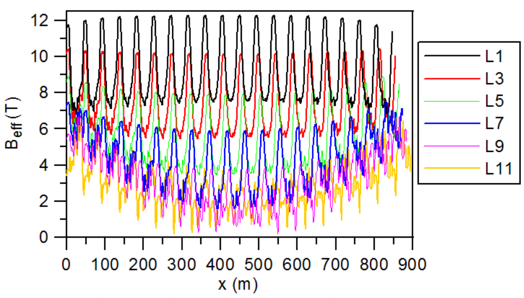

Fig. 4. Magnetic field profiles along the WP#1 cables obtained with M'C.

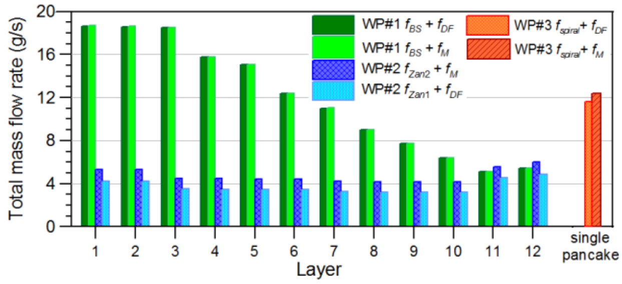

Fig. 5. The maximum and minimum total mass flow rate in each conductor obtained with different pairs of friction factor correlations.

we computed the field profiles using the M'C code from Cryosoft (the results are shown in Fig. 4), whereas for WP#2 the magnetic field data were provided by the ENEA team. From magnetic field maps the T_{cs} (x) profiles along the conductors are calculated using the scaling laws recommended in [23], and $\Delta T^{\min}_{marg}$ is found as the minimum of $\Delta T_{marg}(x) = T_{cs}(x) - T(x)$.

III. Results, Discussion and Conclusions

The main results of the hydraulic analysis are summarized in Fig. 5. The maximum total mass flow rate in the TF coil is assessed to be 144 g/s (WP#1), 57 g/s (WP#2) and 203 g/s (WP#3). These values may serve as a reference for designers of the DEMO cryogenic system. The mass flow rate in WP#2 is much smaller than in WP#1 and 3, which may indicate problems with ΔT_{marg}. The more conservative bundle friction factor correlation, i.e. f_{DF}, is chosen to be applied in the subsequent heat removal analysis.

The results of the heat removal analysis are presented in Figs. 6 – 9. The $\Delta T^{\min}_{marg}$ in the WP#1 and 2 conductors is located at one of the T_{cs} minima in one of the outermost turns (Fig. 6), whereas in the WP#3 conductor it is observed at x_{crit} close to the T_{cs} global minimum in the 1st turn (Fig. 7). In Case **b,** with the highest heat load, x_{crit} is slightly shifted to the right due to the steeper rise of the temperature profile. The $\Delta T^{\min}_{marg}$ values calculated with Q_{NH1} for WP#1 and 3 cables are sufficiently large, except the most pessimistic Case **b** in which $\Delta T^{\min}_{marg}$ is slightly below the 1.5 K acceptance criterion [3], [23]. Applying the new definition of the NH load [17] (Q_{NH2}) leads to reduction of ΔT_{marg} in the WP#1 conductors, which becomes particularly significant in layers L7 - L12. In layers L9 –L12 $\Delta T^{\min}_{marg}$ calculated with Q_{NH2} drops below 1.5 K (Fig 8). Reduction of ΔT_{marg} in the WP#1 cables due to the joint resistance is typically of about 0.02-0.08 K (Fig. 8). The calculated $\Delta T^{\min}_{marg}$ values in some WP#2 cables are slightly too small, particularly when the correlation f_{Zan1} is used. However, more detailed simulations [5], that took into account: inter-turn, inter-layer, and WP-case thermal coupling across the turn and layer insulation, as well as an effective cooling circuit in the case, have shown that the 1.5 K criterion is satisfied also in the potentially problematic layers of WP#2.

The quench simulations in WP#1-3 cables were performed assuming the time between the quench detection t_{delay} = 3.1 s

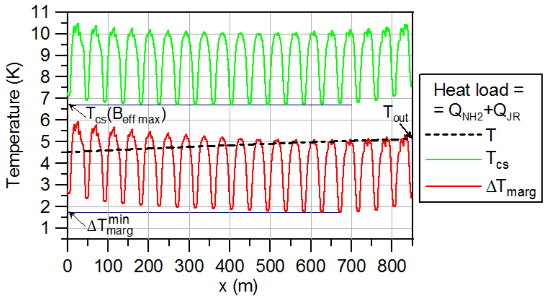

Fig. 6. Temperature, T_{cs} and ΔT_{marg} profiles along the WP#1 L1 cable.

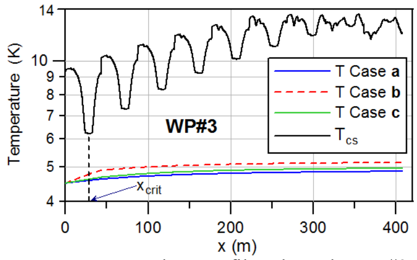

Fig. 7. Temperature and T_{cs} profiles along the WP#3 cable.

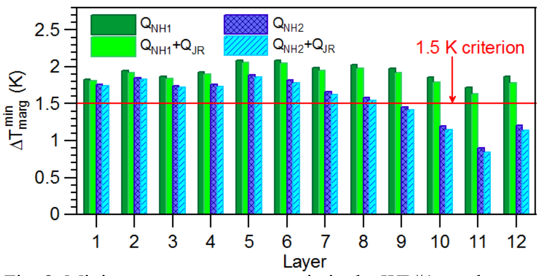

Fig. 8. Minimum temperature margin in the WP#1 conductors.

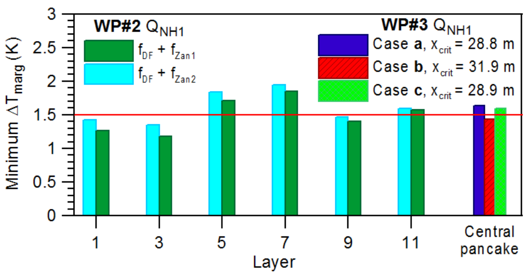

Fig. 9. Minimum temperature margin in the WP#2 and 3 conductors.

and the time constant for the current dump $\tau = 27$ s [23]. In the considered cables the maximum quench temperatures values resulting from our simplified model are in the range 60-110 K, i.e. well below the 150 K ITER criterion [3], [23]. They may serve as a reference (lower limit) for the maximum quench temperatures in case when quench happens simultaneously along the full conductor length.

References

[1] "Fusion Electricity. A roadmap to the realisation of fusion energy," November 2012, Available: https://www.euro-fusion.org/wpcms/wp-content/uploads/2013/01/JG12.356-web.pdf

[2] G. Federici, et al., "Overview of the design approach and prioritization of R&D activities towards an EU DEMO," Fus. Eng. Des., vol. 109–1112016, pp. 1464–1474.

[3] L. Zani, et al., "Overview of Progress on the EU DEMO Reactor Magnet System Design," IEEE Trans. Appl. Supercond., vol. 26, no. 4, Jun. 2016, Art. no. 4204505.

[4] K. Sedlak, P. Bruzzone and M. Lewandowska, "Thermal-hydraulic and quench analysis of the DEMO toroidal field winding pack WP1," Fus. Eng. Des., vol. 124, pp. 110-113, Nov. 2017.

[5] L. Savoldi, et al., "Performance analysis of a graded winding pack design for the EUDEMO TF coil in normal and off-normal conditions," Fusion Eng. Des., vol. 124, pp. 45-48, Nov. 2017.

[6] A. Torre, D. Ciazynski, and L. Zani, "EU-DEMO TF and CS Magnet Systems Design and Analyses Performed at CEA," IEEE Trans. Appl. Supercond., vol. 27, no. 4, Jun. 2017, Art. no. 4900705.

[7] R. Wesche, et al., "Winding pack proposal for the TF and CS coils of European DEMO," IEEE Trans. Appl. Supercond., vol. 26, no. 3, Apr. 2016, Art. no. 4200405.

[8] R. Wesche, et.al, "Central solenoid winding pack design for DEMO," Fusion Eng. Des., vol. 124, pp. 82-85, Nov. 2017..

[9] R. Vallcorba, et al., "Thermohydraulic Analyses on CEA Concept of TF and CS Coils for EU-DEMO," submitted for publication in IEEE Trans. Appl. Supercond., unpublished.

[10] R. Wenninger, Reference Design – 2015 April (EU DEMO1 2015) PROCESS Output, 2015, https://idm.euro-fusion.org/?uid=2MDKFH

[11] M. Lewandowska and K. Sedlak, "Thermal-hydraulic analysis of LTS cables for the DEMO TF coil," IEEE Trans. Appl. Supercond., vol. 24, no. 3, Jun. 2014, Art. no. 4200305.

[12] M. Lewandowska and K. Sedlak, "Thermal-hydraulic analysis of the improved LTS conductor design concepts for the DEMO TF coil," Prz. Elektrotech., vol. 92, no. 4, pp. 179–182, 2016.

[13] M. Lewandowska, K. Sedlak and L. Zani, "Thermal-Hydraulic Analysis of the Low-T_c Superconductor (LTS) Winding Pack Design Concepts for the DEMO Toroidal Field (TF) Coil," IEEE Trans. Appl. Supercond., vol. 26, no. 4, Jun. 2016, Art. no. 4205305.

[14] M. Lewandowska and A. Dembkowska, "Thermal-hydraulic analysis of LTS cables for the DEMO TF coil using simplified models," Nukleonika, vol. 62, no. 1, pp. 23-28, 2017.

[15] R. Vallcorba, et al., "Thermo-hydraulic analyses associated with a CEA design proposal for a DEMO TF conductor," Cryogenics, vol. 80, pp. 317–324, 2016.

[16] L. Zani and U. Fischer, "Advanced definition of neutronic heat load density map on DEMO TF coils," Memo for WPMAG-MCD-2.1/2.2/3.3, 2014, https://idm.euro-fusion.org/?uid=2MFVCA

[17] M. Coleman, "Advanced definition of neutronic heat load density map on DEMO TF coils," Memo for WPMAG-MCD-2.1/2.2/3.3, 2016, https://idm.euro-fusion.org/?uid=2LEFP6

[18] M. Bagnasco, L. Bottura, and M. Lewandowska, "Friction factor correlation for CICC's based on a porous media analogy," Cryogenics, vol. 50, no. 11/12, pp. 711–719, Nov./Dec. 2010.

[19] M. Lewandowska and M. Bagnasco, "Modified friction factor correlation for CICC's based on a porous media analogy," Cryogenics, vol. 51, no. 9, pp. 541–545, Sep. 2011.

[20] R.K. Shah and D.P. Sekulić, "Fundamentals of Heat Exchanger Design," Wiley, New Jersey, 2003 (Table 7.6).

[21] R. Zanino, P. Santagati and L. Savoldi, "Friction factor correltion with application to the central cooling channel of Cable-in-Conduit super-conductors for fusion magnets," IEEE Trans. Appl. Supercond., vol. 10, no. 1, pp. 1066-1069, Mar 2000.

[22] R. Zanino, S. Giors and L. Savoldi Richard, "CFD modeling of ITER cable-in-conduit superconductors. Part III: correlation for the central channel friction factor," Proceedings of the 21 International Cryogenic Engineering Conference (ICEC21), vol. 1, pp. 207-210, 2007.

[23] V. Corato, et al., "Common operating values for DEMO magnets design for 2016," 2016, http://euro- fusionscipub.org/archives/eurofusion/ common-operating-values-for-demo-magnets-design-for-2016-2